Journal of Advanced Engineering Trends
ISSN : 2682 - 2091

Vol.43, No.2. July 2024

http://jaet.journals.ekb.eg

A Comparative Analysis on Different Techniques for Improving the PV System Performance Subjected to Variant Solar Irradiance

Abdelrahman M. Mohamed[(1)] Yehia S. Mohamed [(2)]

Department of electrical engineering, Minia university, Egypt [(1)]
Electrical Engineering Department, Faculty of Engineering, Minia University, Egypt [(2)]
[*]corresponding author abdo_2024@protonmail.com

Abstract

The overall power generated by the photovoltaic system is significantly reduced when the modules are not exposed to equal amounts of solar radiation. Three different approaches of boosting power output under the influence of these circumstances were compared in this study. The three approaches were based on different techniques; static, column reconfiguration, and array reconfiguration. The three methodologies were represented by the TCT, CWR, and RTCT methods, respectively. Each of which proved superior to its counterparts using the same methodology. The three methods were tested in two parts. The first part included five different static shading patterns and have been tested on a 5x5 system. RTCT showed superior results compared to the other two methods. It has improved the power output in the all five patterns with rates ranging between 1.45% and 32.49%. While the CWR method achieved improvement in four patterns with lower percentages (between 1.68% and 27.81%), and one pattern was lower than the static TCT. In the second part, the three methods were tested on a system of one hundred modules, arranged in 10x10 array, and under a dynamic solar radiation pattern that changes over time in ten patterns. RTCT provided the highest improvement rate for all cases with 9.5% for the mean of the total period and CWR achieved 6.9%. Therefore direct development of static systems into array reconfiguration using RTCT is recommended if the goal is to obtain the maximum possible power. Simulations were carried out using MATLAB/Simulink, and the characteristic curves, values of voltages, currents, and power were obtained for each case.

Keywords: *Photovoltaic energy, Partial shading, Total cross tied, Column wise reconfiguration, PV array reconfiguration*

1. Introduction

The continuous rise in global energy demand and the increasing use of fossil fuels as a mean of political and economic pressure, in addition to the escalating harmful effects on the environment, until the world witnessed in the last decade the highest average temperatures in more than a century [1-3], all of these represent some of the today's serious challenges. According to the annual 2022 global climate report, all ten warmest years in the 143-year record have occurred since 2010, with the last nine years (2014-2022) are ranking as the nine warmest years on record [4].

Revised: 15 March, 2023, Accepted: 11 June , 2023

All of this made it necessary for countries to achieve self-sufficiency in their energy needs, especially those that suffer from imbalances and a significant difference between production and consumption. Although this is considered a defect, it is also an opportunity at the same time to rectify the situation through environmentally friendly sources.

Hence, one of the most important options available to make up the shortfall is the widespread use of renewable energy. Solar energy, in particular, is considered one of the best solutions due to its availability throughout the year at a high expectation rate, and it is not tied to a specific place, such as tidal energy and hydroelectric power [5, 6]. It also has the ability to be built in small systems that are integrable with residential homes [7, 8]. As well as the possibility of building large stations in Giga Watts [9]. Despite these advantages, there are still many challenges awaiting development and solutions.

Several studies were presented on how to connect solar energy systems to existing electrical networks [10] and others looked for means to overcome possible environmental conditions such as [11] which focused on the problem of low energy output due to the temperature increase of the system.

From another point of view, to achieve the necessary values of voltage and current, photovoltaic (PV) modules are often connected in a number of series and parallel connections. Under normal conditions, the PV modules get sunlight in an even distribution and there is only one peak in the characteristic P-V curve. When the levels of radiation distributed on the panels vary due to various environmental reasons, such as the accumulation of dust or nearby trees and buildings, or even bird droppings [12] one of the most influential problems arises and it is called partial shading (PS).

PS not only reduces output power but also has the potential to create hotspots. Exposure of one panel to shading not only means that the productivity of the system decreases by the energy amount of this module, but this turns it into a power-consuming unit, which raises the temperature of the panel and exposes it to damage [13]. Bypassing diodes are added to bypass shaded PV cells or modules to safeguard the modules from this effect. However, this addition results in the emergence of multiple peaks in the characteristic curve, making it challenging to extract the maximum power using the conventional tracking approaches. Several methods, including genetic algorithms, cuckoo searches, particle swarm optimization, ant colony optimization, and teaching-learning-based optimization, have been introduced to address this issue [14-15].

Some researchers have focused on developing the internal configuration of the module to improve its ability to combat this phenomenon. For example, article [16] examined the performance of PV modules with different cell bus-bar configurations through analyzing seven types of poly-Si PV cells under PS, it concluded that five bus-bar cells were the most efficient. Article [17] focused on modeling half-cell PV modules under PS using MATLAB software package. Instead of 60 cells in a typical classic PV unit, there are twice as many cells in half-cell modules. Four different cases of partial-shading and one case of no-shading were studied. Unlike others, the authors of [18] investigated how a half-cell module could be used to reduce this PS effect and introduced simulation results with experimentally verification. They concluded that the half-cell module improves fill factor performance by 1.48% due to reduced electrical loss from the cell connector. The module current will also increase by about 3%.

In contrast, other research teams have focused on the system as a whole and how to deal with shadowing for multiple modules within the system [19-20]. They explored different systems under the influence of different PS patterns and tested new methods of static and dynamic linking. Dynamic connection means changing the connection topology at the moment of shading. Table 1 shows a summary of a group of the most important works in this direction

Researchers are currently seeking new innovative methods to maximize the power output during partial shading. The presented methods included static configurations and methods based on reconfiguration either at the column level only or at the entire array level. In the midst of these many creative approaches presented, it is difficult to directly compare them, as each method is presented and tested under different shading levels than presented in the other researches. The test is also conducted on systems with different dimensions that differ from one research to another. Also, the lack of researches that compares static and reconfigurable methods, relying on the same shading patterns for all methods under comparison, and testing these methods on small and relatively large systems, especially as many new approaches emerge.

Table 1. A group of previous important works in this direction

Authors	Interconnection schemes	Configurations	Tested systems size	Irradiance levels (W/m^2)	Achievements	Limitations
Mohammad Nor RAFIQ NAZER et al. [20]	Static only	Series (S), Parallel (P), Series-parallel (SP), Bridge-linked (BL), Honey-comb (HC) and Total-cross-tied (TCT)	3x10, 5x5 and 5x4	300, 500, 700 and 1000	- Covering twenty different shading patterns. - Using six different configurations. - Highlight the differences between the six methods more by testing them on three systems of different sizes. - Finding that the TCT method gives the best performance in general.	- Limited to conventional static methods only. - Only small systems have been tested (less than 30 modules).
G. M. Madhu et al. [19]	Static only	S, P, SP, BL, HC and TCT	4x4	100, 300, 500 and 900	- Covering six different shading patterns with six different static configuration methods. - Verifying simulation results empirically. - The shading patterns cover different radiation levels than usual. - It was concluded that the TCT method had the best performance among the methods under study	- A variable shading pattern has not been tested over a continuous period of time - Only one small model was used for comparison.
Praveen Kumar Bonthagorla and Suresh Mikkili [21]	Static only	-Conventional: SP, TCT, BL, HC and Triple tied (TT) - Hybrid: SP-TCT, BL-TCT, HC-TCT and BL-TCT	7x7	200, 300, 400, 500, 600, 700, 800 and 1000	- Studying nine different methods (five conventional and four hybrid methods). - Simulation with eight different shading patterns. - Measuring the number of local maximum power points and determining the least number of points according to the shading pattern. - Measurement of seven different performance parameters to distinguish between the nine methods.	- Limited to static methods only. - A variable shading pattern has not been tested over a continuous period of time
Mustapha Elyaqouti et al. [22]	Static only	S, P, SP, TCT, BL, and HC	5x4	200, 400, 600, 800 and 1000	- Six conventional static configurations were studied under five different shading patterns. - When a column is completely and unevenly shaded, TCT is the best choice.	- It is limited to traditional static methods only. - Limited shading patterns.

Karmakar and Gopinath Karmakar	Static and reconfigurable.	TCT	4x3	180 to 1000	- This paper presented a new method which avoided the existence of multiple peaks on the PV characteristic curve through current injection using power electronics. - The method is combined with static TCT configuration.	- The power converters circuit had to be modified. - Complex algorithm.
A. Srinivasan et al. [24]	Reconfigurable	L-shaped	4x4	100, 400, 600, 800 and 950	- A new method based on reshaping the array connections to be in the form of the letter "L". - Eight overlaid shading patterns with extraordinary radiation levels.	- A variable shading pattern has not been tested over a continuous period of time. - It needs an equal-dimensional system
Rupendra Kumar Pachauri et al. [25]	Static and reconfigurable.	LS-TCT Shape-do-ku	4x4	300, 500 and 1000	- Two new methods have been introduced (the first was a static method and the second was a reconfigurable one) - The results were verified experimentally and the methods were compared with TCT and Su-Du-Ku methods.	- Relatively complex reconfiguration process. - Only one small system was used for testing the method.
Abdelrahman M. Mohamed et al. [26]	Static and reconfigurable.	Reconfigurable total cross tied (RTCT)	2x3, 2x4, 2x5, 2x2 and 3x3	300 and 1000	- Covered all possible shading patterns for one level of shading. - Covered all systems that can be configured with ten modules or less. - Focused study on small-scale systems. - Introduced the RTCT method and measuring its performance.	- Limited to small-scale systems only. - Studied only two levels of solar radiation.
J. Prasanth Ram et al. [27]	Static and reconfigurable-column	Column-wise reconfiguration (CWR)	5x5	200, 500, 600 and 900	- Presented a new method based on in-column reshaping only. - Creatively relying on the deployment of aggregated shaded modules across the entire system.	- Has not been compared with another reconfigurable methods.
Aidha Muhammad Ajmal et al. [28]	Static and reconfigurable	Review on more than 36 methods	---	---	- More than 36 methods including both fixed and reconfigurable methods are demonstrated and discussed.	- Not all methods have been tested on a system with the same dimensions and under the same shading patterns - Column-wise reconfigurations have not been included.

Bo Yang et al. [29]	Static and reconfigurable	Review on more than 64 methods have been introduced until 2020 New method based on Social-democratic algorithm.	10x10	100, 200, 300, 400, 500, 600, 700, 800, 900 and 1000	- Providing a good review of many methods that have been presented (64 methods) up to 2020. - Introducing a new method that reshapes the system based on the optimal performance method based on the social-democratic algorithm. - Coverage of shading occurrence over a continuous period of time that included ten different shading patterns. - Comparison of ten methods based on meta-heuristic algorithms..	- No comparison was made with the column reconfiguring method.
Mariana Durango-Flórez et al. [30]	Reconfigurable	Reconfigurable based on Genetic algorithm (GA)	6x3	50% and 100%	- It is based on Genetic algorithm - GA switches between SP and TCT to get the best performance between them according to the shading pattern	- Not compared with other reconfigurable methods and only compared with static methods. - Using only two shading patterns to test the method with only one shading radiation level. - Complex and does not necessarily reach the best possible performance.
Vinaya Chandrakant Chavan et al. [31]	Reconfigurable	Reconfigurable NSD method	6x6	200, 500, 700 and 1000	- Introduced a new method and tested it under nine different shading patterns. - Not restricted to specific dimensions, such as the Su-Du-Ku method, which requires a 9x9 system. - The proposed method showed higher performance in most of the studied shading patterns.	- Not compared with other reconfigurable methods and only compared with static methods. - A variable shading pattern has not been tested over a continuous period of time.
This paper	Static and reconfigurable	TCT RTCT CWR	5x5 and 10x10	Static 200, 500, 600 and 900 and dynamic from 100 to 1000	What's new in research is: - Comparison of three methods belonging to the three different configurations (fixed - reconfigurable at the column level and at the total array level). - The three techniques are simulated under four fixed different shading patterns as well as a time-varying shading case containing ten different patterns. - The comparison was made at the level of the small system 4x4 and the relatively large-10x10 system. - Recommendations are provided on upgrading photovoltaic systems from static to reconfigurable with the enhanced improvement rates.	

2. Mathematical Modeling

The solar cell can be modelled in a variety of ways, including the single diode model (SDM), double diode model, and triple diode model. SDM presents a reasonable level of simplicity and a respectable level of accuracy [20]. Figure 1 shows the analogous circuit for SDM.

The module voltage, thermal voltage, series and parallel resistance, and diode ideality factor are all related to the PV cell's current in the following formulas:

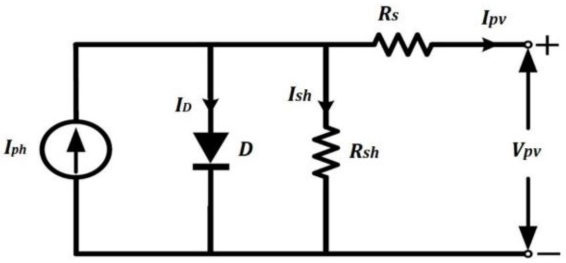

Figure 1. Single diode model

$$I_{pv} = I_{ph} - I_0\left(e^{\frac{V_{pv}+I_{pv}R_s}{aV_t}} - 1\right) - \frac{V_{pv}+I_{pv}R_s}{R_{sh}} \quad (1)$$

Where:

I_{PV}	output current of the PV cell
I_0	reverse saturation current
I_{ph}	light generated current
V_t	thermal voltage
K	Boltzmann's constant
N_S	number of series cells
G	solar irradiance
I_{SC}	short circuit current
K_V	temperature voltage coefficient
a	diode ideality factor
R_S	series resistance
R_{sh}	shunt resistance
T	absolute temperature in Kelvins
q	electron charge
K_i	temperature coefficient of short circuit current
T_{STC}	reference temperature
V_{OC}	open circuit voltage
STC	Standard test conditions: G_{STC} = 1000 W/m^2, air mass ratio = 1.5, and temperature of the module = 25 °C

The module's thermal voltage is indicated by:

$$V_t = \frac{KTN_s}{q} \quad (2)$$

The amount of irradiance has a direct impact on the generated current, as

$$I_{ph} = (I_{SC,STC} + K_i(T - T_{STC})) * \frac{G}{G_{STC}} \quad (3)$$

Finally, it is possible to extract the reverse saturation current from

$$I_0 = \frac{I_{SC,STC} + K_i(T - T_{STC})}{e^{\frac{V_{pv}+I_{pv}R_s}{aV_t}} - 1} \quad (4)$$

3. Methodology:

The unevenness of solar radiation on all modules in the system severely reduces the value of the power produced. Several configurations have been presented in the literature to improve the solar energy system performance under these conditions. Static configurations are characterized by not using switches. The TCT configuration has proven to be superior to many other static methods.

Other techniques tended to reposition the shaded module within the same column it was in. So that, the column is reconfigured without moving the shaded module to another column. Among the most recent methods presented in this field is the column-wise-reconfiguration (CWR) method, which has proven to improve the performance of the solar energy system. In this method, each module is numbered by row and column numbers. This number is then squared, and the module moves a number of steps according to the squared result. If the result of the square is a number with more than one digit, then the digits are added together to produce the new moving single-digit number. After moving the module, if the new location the module is moved to is reserved by another module, it will be kept in the save box. After completing the repositioning of all modules, the modules in the save box are placed in the remaining vacant places. A more detailed explanation of the method is available in [27].

Other reconfiguration methods focused on reconfiguring the entire system so that the shaded module could be moved to any row or column. The researchers in [16] introduced a unique reconfiguration method called reconfigurable total cross tied (RTCT). This method relied on the descending order of the shaded modules from the most shaded to the least shaded, and the arrangement starts from the nearest corner. The second column starts from where the first column ended. This method has been tested on more than a hundred shading patterns applied to five systems of different dimensions and showed a remarkable improvement in the output power value under the majority of shading patterns.

In this study, a comparison are investigated between the three methods of static, column reconfiguration, and array reconfiguration represented by the TCT, CWR, and RTCT methods, respectively. The three methods are tested in two parts. The first part involves static shading patterns, and the system are tested under five different shading patterns on a 5x5 system as shown in Figure 2.

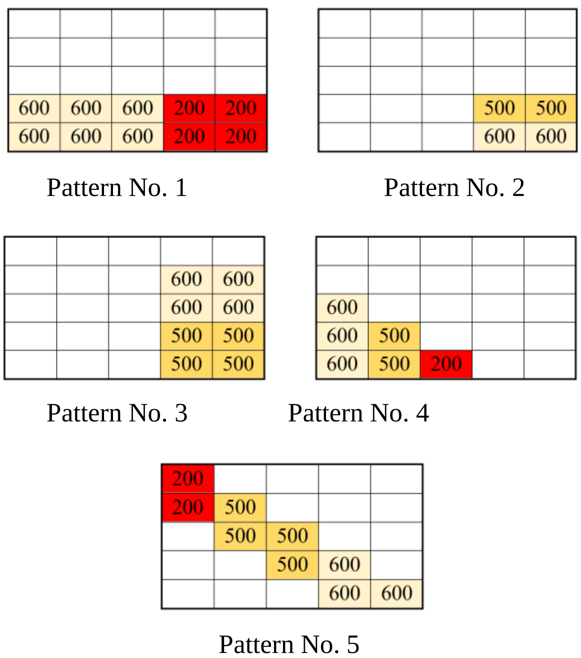

Figure 2. Static shading patterns

Three levels of radiation are approved; the first is the full radiation and represented by 900 W/m^2, the second is medium radiation which represented by 500 and 600 W/m^2, and the third is weak radiation and represented by 200 W/m^2. As shown in the literature review table, there is no specific standard for representing radiation levels, but the main criterion is to cover the gradation of different radiation levels.

In the second part, the three methods are tested on a system of one hundred modules, arranged in 10x10 array, and under a dynamic solar radiation pattern that changes over time in ten patterns. Radiation levels started from 1000 W/m^{2}and decreased to 100 W/m^{2}at a rate of 100 W/m^2, so that the system is exposed to ten different radiation levels at the same time. This dynamic pattern was derived from the review [29] and Figure 3 illustrates it.

The percentage of improvement compared to the first method is measured through the equation:

$$Improvement\ ratio\ (IR\%) = \frac{P_{method} - P_{TCT}}{P_{TCT}} * 100\ \%$$

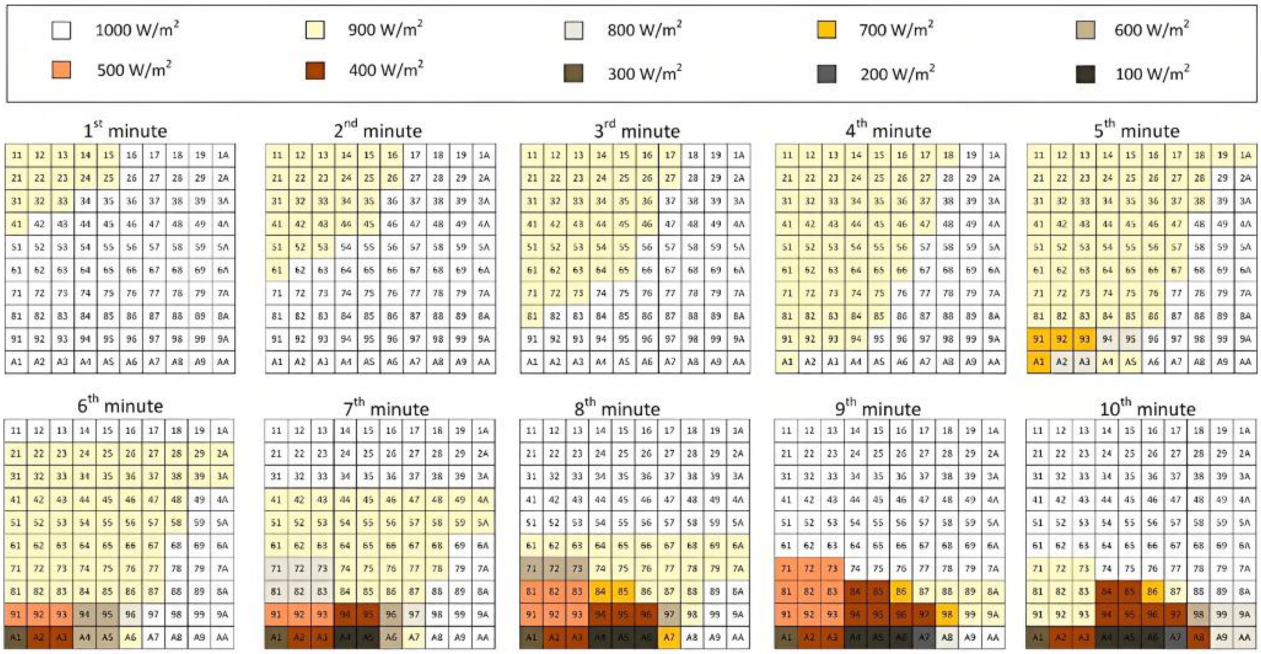

Figure 3. Dynamic shading pattern [29]

4. Results and discussions:

A comparison is investigated between the three selected methods, each of which proved superior to its counterparts using the same methodology. Two selected systems were built using Suntech Power STP300-24/Vd module. Simulations were carried out using MATLAB/Simulink, and the VOC, ISC, VMP, IMP and PMP values were extracted, as well as characteristic curves for each case.

In the first part, the 5x5 system was exposed to five static shading patterns as follows:

Pattern No. 1:

This pattern represents the shading of entire rows with varying shading levels. A solar radiation of 900 W/m^2 is considered for the unshaded modules and two degrees of shading are applied with values of 600 and 200 W/m^2.

600	600	600	200	200
600	600	600	200	200

(a) TCT

		600		
600	600			200
	600			200
600			200	
		600	200	

(b) CWR

200	600			
200	600			
200	600			
200	600			
600	600			

(c) RTCT

Figure 4. Techniques response to pattern No.1

			500	500
			600	600

(a) TCT

				600
				500
			600	
			500	

(b) CWR

				600
				600
				500
				500

(c) RTCT

Figure 5. Techniques response to pattern No.2

(a) TCT

			600	600
			600	600
			500	500
			500	500

(b) CWR

			600	600
			600	500
				500
			500	600
			500	

(c) RTCT

				500
				500
			600	500
			600	500
			600	600

Figure 6. Techniques response to pattern No.3

(a) TCT

600				
600	500			
600	500	200		

(b) CWR

		200		
600	500			
600	500			
600				

(c) RTCT

200				
500				
500				
600				
600	600			

Figure 7. Techniques response to pattern No.4

(a) TCT

200				
200	500			
	500	500		
		500	600	
			600	600

(b) CWR

200	500			
		500		600
	500		600	
200		500	600	

(c) RTCT

200				
200	600			
500	600			
500	600			
500	500			

Figure 8. Techniques response to pattern No.5

Figure 4 shows the response of each of the three methods as a result of exposure to the shading pattern. CWR achieved an improvement rate of 27.81%, while RTCT provided the highest improvement rate of about 32.49%. Both methods also provided an acceptable level of voltage and current values compared to TCT. Figure 9 shows the characteristic curves of the three methods under the influence of this pattern.

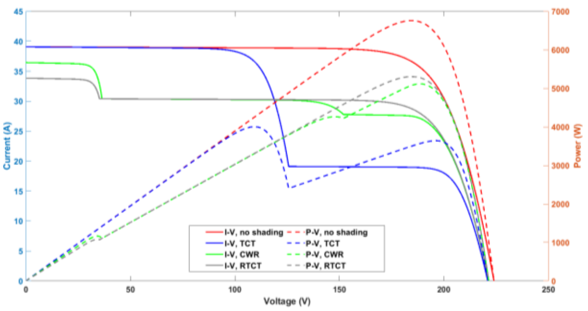

Figure 9. (I-V) and (P-V) characteristic curves of the PV system under shading pattern No. 1

Pattern No. 2:

Pattern No. 2 expresses the occurrence of shading in the corner. This is represented by the shading of two close levels of 500 and 600 W/m^2. The locations of the new shaded modules after applying the three methods are shown in Figure 5. CWR and RTCT methods achieved an equal improvement of 5.1% compared to TCT. Figure 10 shows the power and current versus voltage curves.

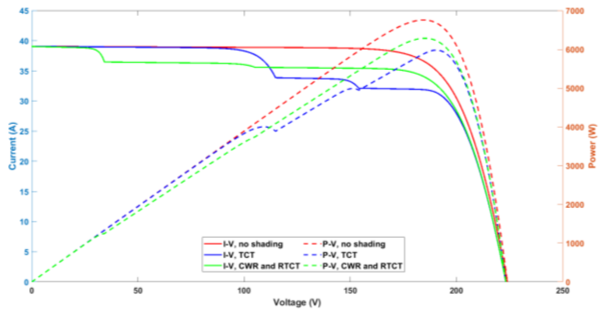

Figure 10. (I-V) and (P-V) characteristic curves of the PV system under shading pattern No. 2

Pattern No. 3:

Longitudinal shading is possible, so it was taken into account in this pattern. Shading of two adjacent columns with two different levels of solar radiation was considered. The places of the modules are reconfigured based on the three methods to become as shown in Figure 6. It is noted here that both reconfiguration methods are equal in the amount of power, voltage and current values as shown by the curves in Figure 11. And the improvement was 1.68% (with a power increase of 96.6 W) comparing with TCT.

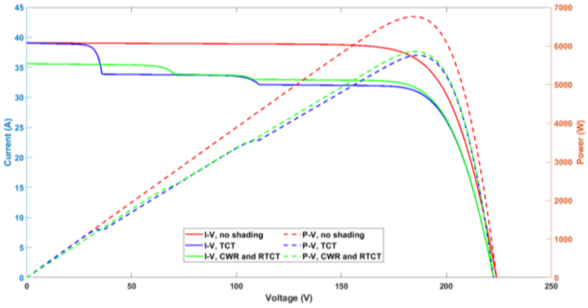

Figure 11. (I-V) and (P-V) characteristic curves of the PV system under shading pattern No. 3

Pattern No. 4:

Pattern 4 represents three different shades of 200, 500, and 600 W/m^2. The system is exposed to them in a gradual, ladder-like manner, while the rest of the modules have an equal radiation rate of 900 W/m^2. Figures 7 and 12 show the new shape after reconfiguring the array and the characteristic curves, respectively.

RTCT provided the highest improvement rate of 15.15% with a power increase of 782.9 W, while CWR was second with an improvement rate of 13.66%. Both methods provided acceptable levels of VMP and IMP.

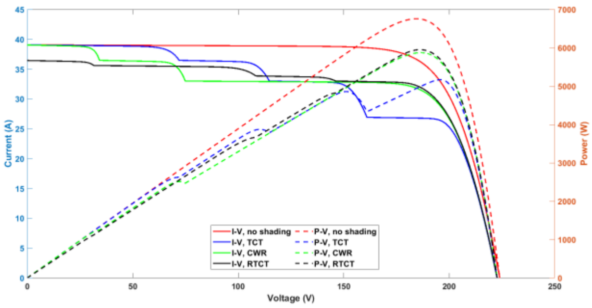

Figure 12. (I-V) and (P-V) characteristic curves of the PV system under shading pattern No. 4

Pattern No. 5:

This pattern takes into account diagonal shading. It is represented by three levels of shading (200, 500 and 600 w/m^2) that occupy the diagonal of the array. Figure 8 shows the response of each method and Figure 13 indicates the characteristic curves of the three compared methods with the no-shading case. RTCT method achieved an improvement of 1.45% compared to TCT. Also, it is important to note here that CWR has a negative improvement by -6.6% which means that static TCT is better than CWR.

The results of all measured values, along with the percentage of improvement, are recorded in Table 2. The no-shading case represents equal radiation on all modules with a value of 900 W/m^2. For further explanation, the resulting power values are plotted under each shading pattern in the bar graph shown in Figure 14.

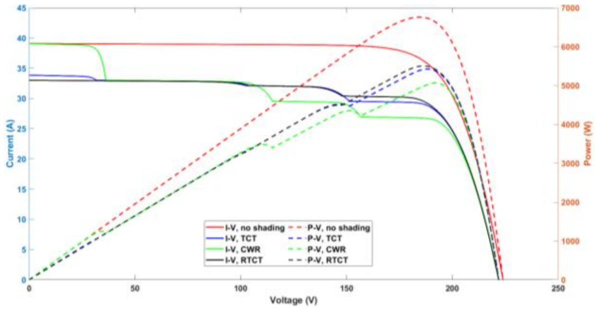

Figure 13. (I-V) and (P-V) characteristic curves of the PV system under shading pattern No. 5

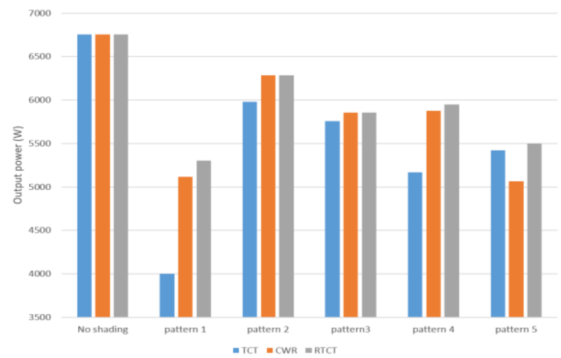

Figure 14. Bar chart of the three techniques' output power under the shading patterns

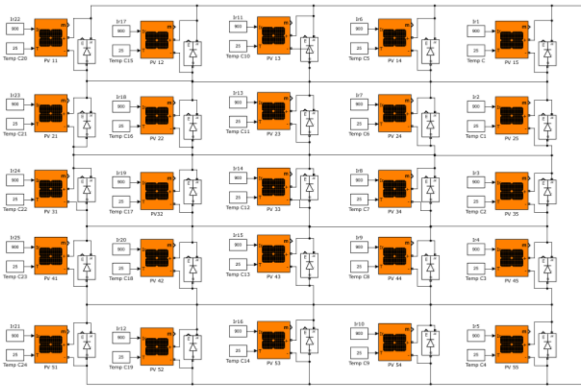

Figure 15. The 5x5 system showing the bypassing diodes

Table 2. Output values measured under different shading patterns

	Method	V_{OC} (V)	I_{SC} (A)	V_{MP} (V)	I_{MP} (A)	P_{MP} (W)	IR%
No-shading	All	223.9	39.08	184.41	36.64	6757.5	---
Pattern No. 1	TCT	220.9	39.08	109.31	36.62	4003.0	---
	CWR	221.4	36.48	188.55	27.14	5116.4	27.81%
	RTCT	221.4	33.87	184.55	28.74	5303.4	32.49%
Pattern No. 2	TCT	223.2	39.08	190.40	31.41	5980.4	---
	CWR	223.2	39.08	185.13	33.95	6285.6	5.1%
	RTCT	223.2	39.08	185.09	33.96	6285.6	5.1%
Pattern No. 3	TCT	222.4	39.08	186.44	30.88	5756.9	---
	CWR	222.5	35.61	185.31	31.59	5853.5	1.68%
	RTCT	222.5	35.61	185.31	31.59	5853.5	1.68%
Pattern No. 4	TCT	222.6	39.08	195.62	26.42	5168.2	---
	CWR	222.7	39.08	186.48	31.50	5874.4	13.66%
	RTCT	222.7	36.48	186.08	31.98	5951.1	15.15%
Pattern No. 5	TCT	221.8	33.87	188.06	28.83	5421.5	---
	CWR	221.8	39.08	192.02	26.37	5063.5	-6.6%
	RTCT	221.8	33.00	186.17	29.55	5501.1	1.45%

For further analysis, the activation of the bypass diodes within the system was studied under the conditions of the five patterns. Figure 15 shows the system, with bypass diodes numbered from D11 to D55. The bypass diodes were recorded in the state of activation; through which a current is passing, and simulated under the application of the three methods. It is noticed that the row with the least shading, (with the highest radiation), contains the non-activated bypass diode. And if two rows have equal total radiation summation, the bypass diodes of the two rows are not activated. It is also noted that all the bypass diodes in the same row are subject to the same conditions for activation or not, due to the TCT connection which makes all the bypass diodes in the same row have the same voltage at both ends. The two methods, CWR and RTCT, have activated more of these diodes, which means more ability to pass current outside the shaded modules, which means higher power output in the end.

Table 3. Bypassing diodes activation states

	TCT					CWR					RTCT				
P1	D11	D12	D13	D14	D15	D11	D12	D13	D14	D15	D11	D12	D13	D14	D15
	OFF	**OFF**	**OFF**	**OFF**	**OFF**	**OFF**	**OFF**	**OFF**	**OFF**	**OFF**	**ON**	**ON**	**ON**	**ON**	**ON**
	D21	D22	D23	D24	D25	D21	D22	D23	D24	D25	D21	D22	D23	D24	D25
	OFF	**OFF**	**OFF**	**OFF**	**OFF**	**ON**	**ON**	**ON**	**ON**	**ON**	**ON**	**ON**	**ON**	**ON**	**ON**
	D31	D32	D33	D34	D35	D31	D32	D33	D34	D35	D31	D32	D33	D34	D35
	OFF	**OFF**	**OFF**	**OFF**	**OFF**	**ON**	**ON**	**ON**	**ON**	**ON**	**ON**	**ON**	**ON**	**ON**	**ON**

	D41	D42	D43	D44	D45	D41	D42	D43	D44	D45	D41	D42	D43	D44	D45
	ON	**ON**	**ON**	**ON**	**ON**	**ON**	**ON**	**ON**	**ON**	**ON**	**ON**	**ON**	**ON**	**ON**	**ON**
	D51	D52	D53	D54	D55	D51	D52	D53	D54	D55	D51	D52	D53	D54	D55
	ON	**ON**	**ON**	**ON**	**ON**	**ON**	**ON**	**ON**	**ON**	**ON**	**OFF**	**OFF**	**OFF**	**OFF**	**OFF**
P2	D11	D12	D13	D14	D15	D11	D12	D13	D14	D15	D11	D12	D13	D14	D15
	OFF	**OFF**	**OFF**	**OFF**	**OFF**	**OFF**	**OFF**	**OFF**	**OFF**	**OFF**	**OFF**	**OFF**	**OFF**	**OFF**	**OFF**
	D21	D22	D23	D24	D25	D21	D22	D23	D24	D25	D21	D22	D23	D24	D25
	OFF	**OFF**	**OFF**	**OFF**	**OFF**	**ON**	**ON**	**ON**	**ON**	**ON**	**ON**	**ON**	**ON**	**ON**	**ON**
	D31	D32	D33	D34	D35	D31	D32	D33	D34	D35	D31	D32	D33	D34	D35
	OFF	**OFF**	**OFF**	**OFF**	**OFF**	**ON**	**ON**	**ON**	**ON**	**ON**	**ON**	**ON**	**ON**	**ON**	**ON**
	D41	D42	D43	D44	D45	D41	D42	D43	D44	D45	D41	D42	D43	D44	D45
	ON	**ON**	**ON**	**ON**	**ON**	**ON**	**ON**	**ON**	**ON**	**ON**	**ON**	**ON**	**ON**	**ON**	**ON**
	D51	D52	D53	D54	D55	D51	D52	D53	D54	D55	D51	D52	D53	D54	D55
	ON	**ON**	**ON**	**ON**	**ON**	**ON**	**ON**	**ON**	**ON**	**ON**	**ON**	**ON**	**ON**	**ON**	**ON**
P3	D11	D12	D13	D14	D15	D11	D12	D13	D14	D15	D11	D12	D13	D14	D15
	OFF	**OFF**	**OFF**	**OFF**	**OFF**	**ON**	**ON**	**ON**	**ON**	**ON**	**OFF**	**OFF**	**OFF**	**OFF**	**OFF**
	D21	D22	D23	D24	D25	D21	D22	D23	D24	D25	D21	D22	D23	D24	D25
	ON	**ON**	**ON**	**ON**	**ON**	**ON**	**ON**	**ON**	**ON**	**ON**	**OFF**	**OFF**	**OFF**	**OFF**	**OFF**
	D31	D32	D33	D34	D35	D31	D32	D33	D34	D35	D31	D32	D33	D34	D35
	ON	**ON**	**ON**	**ON**	**ON**	**OFF**	**OFF**	**OFF**	**OFF**	**OFF**	**ON**	**ON**	**ON**	**ON**	**ON**
	D41	D42	D43	D44	D45	D41	D42	D43	D44	D45	D41	D42	D43	D44	D45
	ON	**ON**	**ON**	**ON**	**ON**	**ON**	**ON**	**ON**	**ON**	**ON**	**ON**	**ON**	**ON**	**ON**	**ON**
	D51	D52	D53	D54	D55	D51	D52	D53	D54	D55	D51	D52	D53	D54	D55
	ON	**ON**	**ON**	**ON**	**ON**	**OFF**	**OFF**	**OFF**	**OFF**	**OFF**	**ON**	**ON**	**ON**	**ON**	**ON**
P4	D11	D12	D13	D14	D15	D11	D12	D13	D14	D15	D11	D12	D13	D14	D15
	OFF	**OFF**	**OFF**	**OFF**	**OFF**	**ON**	**ON**	**ON**	**ON**	**ON**	**ON**	**ON**	**ON**	**ON**	**ON**
	D21	D22	D23	D24	D25	D21	D22	D23	D24	D25	D21	D22	D23	D24	D25
	OFF	**OFF**	**OFF**	**OFF**	**OFF**	**ON**	**ON**	**ON**	**ON**	**ON**	**ON**	**ON**	**ON**	**ON**	**ON**
	D31	D32	D33	D34	D35	D31	D32	D33	D34	D35	D31	D32	D33	D34	D35
	ON	**ON**	**ON**	**ON**	**ON**	**ON**	**ON**	**ON**	**ON**	**ON**	**ON**	**ON**	**ON**	**ON**	**ON**
	D41	D42	D43	D44	D45	D41	D42	D43	D44	D45	D41	D42	D43	D44	D45
	ON	**ON**	**ON**	**ON**	**ON**	**ON**	**ON**	**ON**	**ON**	**ON**	**OFF**	**OFF**	**OFF**	**OFF**	**OFF**
	D51	D52	D53	D54	D55	D51	D52	D53	D54	D55	D51	D52	D53	D54	D55
	ON	**ON**	**ON**	**ON**	**ON**	**OFF**	**OFF**	**OFF**	**OFF**	**OFF**	**ON**	**ON**	**ON**	**ON**	**ON**
P5	D11	D12	D13	D14	D15	D11	D12	D13	D14	D15	D11	D12	D13	D14	D15
	ON	**ON**	**ON**	**ON**	**ON**	**ON**	**ON**	**ON**	**ON**	**ON**	**OFF**	**OFF**	**OFF**	**OFF**	**OFF**
	D21	D22	D23	D24	D25	D21	D22	D23	D24	D25	D21	D22	D23	D24	D25
	ON	**ON**	**ON**	**ON**	**ON**	**ON**	**ON**	**ON**	**ON**	**ON**	**ON**	**ON**	**ON**	**ON**	**ON**
	D31	D32	D33	D34	D35	D31	D32	D33	D34	D35	D31	D32	D33	D34	D35
	ON	**ON**	**ON**	**ON**	**ON**	**OFF**	**OFF**	**OFF**	**OFF**	**OFF**	**OFF**	**OFF**	**OFF**	**OFF**	**OFF**
	D41	D42	D43	D44	D45	D41	D42	D43	D44	D45	D41	D42	D43	D44	D45
	ON	**ON**	**ON**	**ON**	**ON**	**ON**	**ON**	**ON**	**ON**	**ON**	**OFF**	**OFF**	**OFF**	**OFF**	**OFF**
	D51	D52	D53	D54	D55	D51	D52	D53	D54	D55	D51	D52	D53	D54	D55
	OFF	**OFF**	**OFF**	**OFF**	**OFF**	**ON**	**ON**	**ON**	**ON**	**ON**	**ON**	**ON**	**ON**	**ON**	**ON**

In the second part, the 10x10 system was exposed to a dynamic shading patterns as shown in Figure 3. The patterns changed over time in ten different shapes. The results recorded for each shape and the average are shown in Table 4 where the output power without and shading equals 30032 W. RTCT provided the highest improvement rate for all cases with 9.5% for average of the total period where CWR achieved 6.9%.Also, it is observed that the effectiveness of the two methods increased mainly with increasing the shading depth. In the first five minutes, the improvement rate did not exceed 1% as the shading depth was small. CWR and RTCT presented an improvement rate with priority to RTCT of 2.6% comparing to CWR.

Then in the next five minutes, the shading depth was more. So, the improvement rates were higher. For example, in the 9th minute, RTCT and CWR achieved rates of 30.56% and 23.95% respectively. That means more than 5.9 KW for RTCT and that's a rich plus.

Table 4. Output values measured under different shading patterns

No.	TCT (W)	CWR (W)	RTCT (W)	CWR IR%	RTCT IR%
1	29477	29563	29605	0.29	0.43
2	29077	29211	29245	0.46	0.58
3	28667	28792	28831	0.43	0.57

4	28271	28310	28344	0.14	0.26
5	27419	27493	27583	0.27	0.60
6	24056	25534	26680	6.14	10.91
7	22085	25570	26259	15.78	18.90
8	20149	24523	25600	21.71	27.05
9	19358	23994	25274	23.95	30.56
10	21458	24276	26335	13.13	22.73
Average	25002	26727	27376	6.90	9.50

6. Conclusion

When the modules of the PV system are not exposed to equal amounts of solar radiation, the value of the total power produced by the system is greatly reduced. In this study, a comparison was made between three methods to increase the power output under the influence of these conditions. The three methods are based on different techniques: static, reconfiguring the column, and reconfiguring the array. The TCT, CWR, and RTCT methods were chosen to represent the three techniques, respectively. The three methods were tested in two parts. The first part included five different static shading patterns and have been tested on a 5x5 system. RTCT showed superior results compared to the other two methods. It improved power output in all five patterns with rates ranging from 1.45% to 32.49%. While the CWR method achieved improvement in four patterns with lower percentages ***(***between 1.68% and 27.81%***)***, and one pattern was lower than the static TCT. Therefore, direct development of static systems into array reconfiguration using RTCT is recommended if the goal is to obtain the maximum possible power. The effect of the three methods on the diodes was also studied, and it was found that the two methods, RTCT and CWR, activated a larger number of bypassing diodes, which gives a greater opportunity for the string currents to pass outside the shaded modules and then a higher output capacity was produced.

In the second part, the three methods were tested on a system of one hundred modules, arranged in a 10x10 array, and under a dynamic solar radiation pattern that changes over time in ten patterns. RTCT provided the highest improvement rate for all cases with 9.5% for the average of the total period where CWR achieved 6.9%. It was also noticed that the effectiveness of the two methods increased mainly with increasing the shading depth.

For future work:

1. Innovating new methods based on metaheuristics techniques
2. Conducting an extensive study to calculate the value for money resulting from the development of the system using the three methods under study.
3. Studying the losses resulting from switches using different reconfigurable methods and how to increase the speed of changing the connection
4. Integration of artificial intelligence and machine learning techniques to innovate methods that can understand the nature of shading in the area and try to predict the shading pattern and determine the optimum method to achieve the highest performance.

REFERENCES

[1] Harro van Asselt, Peter Newell. Pathways to an International Agreement to Leave Fossil Fuels in the Ground. Global Environmental Politics; 22 (4): 28–47, 2022.

[2] Peng Song, Xianqiang Mao, Ziyan Li, Zhixiong Tan. Study on the optimal policy

options for improving energy efficiency and Co-controlling carbon emission and local air pollutants in China. Renewable and Sustainable Energy Reviews, 175, 113167, 2023.

[3] Sigrid J. Bakke, Monica Ionita, and Lena M. Tallaksen. Recent European drying and its link to prevailing large-scale atmospheric patterns. Published online on researchsquare.com, retrieved on January 6, 2023. doi:10.21203/rs.3.rs-2397739/v1

[4] NOAA National Centers for Environmental Information, Monthly Global Climate Report for Annual 2022. published online January 2023, retrieved on January 27, 2023 from https://www.ncei.noaa.gov/access/monitoring/monthly-report/global/202213.

[5] Konduru Sudharshan, C. Naveen, Pradeep Vishnuram, Damodhara Venkata, Siva Krishna Rao Kasagani, Benedetto Nastasi. Systematic Review on Impact of Different Irradiance Forecasting Techniques for Solar Energy Prediction. Energies, 15 (17), 6267, 2022.

[6] Montaser Abd El Sattar1, Kenawy Ahmed, Alaa AboZied, Ahmed A. Zaki Diab. Adaptive MPPT of Water Photovoltaic Pumping System Based on Vector Controlled Induction Motor Drives. Journal of Advanced Engineering Trends, 41 (2), 261-274, 2021.

[7] David Restrepo-Herrera, Walter Martinez, Luz Adriana Trejos-Grisales, Bonie Johana Restrepo-Cuestas. A Holistic Approach for Design and Assessment of Building-Integrated Photovoltaics Systems. Applied Sciences, 13 (2), 746, 2023.

[8] Sepehr Shahgholian, Mahdi Taheri, Mehdi Jahangiri. Investigating the Cost-Effectiveness of Solar Electricity Compared to Grid Electricity in the Capitals of Middle Eastern Countries: A Residential Scale Case Study. International Journal of Photoenergy, vol. 2023, 8028307, 19 pages, 2023.

[9] Shiwei Yu, Ruilian Han, Junjie Zhang, Reassessment of the potential for centralized and distributed photovoltaic power generation in China: On a prefecture-level city scale. Energy, 262 (A), 125436, 2023.

[10] Semich Impram, Secil Varbak Nese, Bülent Oral. Challenges of renewable energy penetration on power system flexibility: A survey. Energy Strategy Reviews, 31, 100539, 2020.

[11] T. Nordmann and L. Clavadetscher. Understanding temperature effects on PV system performance. 3rd World Conference on Photovoltaic Energy Conversion, Proceedings of, Osaka, Japan, 3, 2243-2246, 2003.

[12] H. S. Sahu, S. K. Nayak and S. Mishra. Maximizing the Power Generation of a Partially Shaded PV Array. IEEE Journal of Emerging and Selected Topics in Power Electronics, 4 (2), 626-637, 2016.

[13] Shenshen Zhao, Haiyong Chen, Chuhan Wang, Shijie Shi. SNCF-Net: Scale-aware neighborhood correlation feature network for hotspot defect detection of photovoltaic farms. Measurement, 206, 112342, 2023.

[14] Ashish Raj, Manoj Gupta. Numerical Simulation and Comparative Assessment of Improved Cuckoo Search and PSO based MPPT System for Solar Photovoltaic System Under Partial Shading Condition. Turkish Journal of Computer and Mathematics Education (TURCOMAT). 12(6), 3842-3855. 2021.

[15] Abdelrahman M. Mohamed, Abou-Hashima M. El-Sayed, Yehia S. Mohamed, Husam A. Ramadan. ENHANCEMENT OF PHOTOVOLTAIC SYSTEM PERFORMANCE BASED ON DIFFERENT ARRAY TOPOLOGIES UNDER PARTIAL SHADING CONDITIONS. Journal of Advanced Engineering Trends. 40 (1), 49-62, 2021.

[16] Youssef MAM, Abdelrahman M. Mohamed, Yaser A. Khalaf, Yehia S. Mohamed. Investigation of Small-Scale Photovoltaic Systems for Optimum Performance under Partial Shading Conditions. Sustainability. 14 (6),3681, 2022.

[17] Mariusz T. Sarniak. Modeling the Functioning of the Half-Cells Photovoltaic Module under Partial Shading in the Matlab Package. Applied Sciences. 10 (7), 2575, 2020.

[18] Hamed Hanifi, Jens Schneider, Joerg Bagdahn. Reduced Shading Effect on Half-Cell Modules—Measurement and Simulation. In Proceedings of the 31st European Photovoltaic Solar Energy Conference and Exhibition, Hamburg, Germany, 14–18 September 2015؛ 2529–2533, 2023.
[19] G. M. Madhu, C. Vyjayanthi , Chirag N. Modi. Investigation on Effect of Irradiance Change in Maximum Power Extraction From PV Array Interconnection Schemes During Partial Shading Conditions. IEEE Access. 9, 96995-97009, 2021.
[20] Mohammad Nor RAFIQ NAZER, Abdulfattah NOORWALI, Mohammad Faridun Naim TAJUDDIN, Mohammad Zubair KHAN, et al. Scenario-Based Investigation on the Effect of Partial Shading Condition Patterns for Different Static Solar Photovoltaic Array Configurations. IEEE Access. 9, 116050-116072, 2021.
[21] Praveen Kumar Bonthagorla; Suresh Mikkili, Performance investigation of hybrid and conventional PV array configurations for grid-connected/standalone PV systems. CSEE Journal of Power and Energy Systems. 8 (3), 682-695, 2022.
[22] Mustapha Elyaqouti, Driss Izbaim, Lahoussine Bouhouch. Study of the Energy Performance of Different PV Arrays Configurations Under Partial Shading. E3S Web of Conferences, 229;01044, 2021.
[23] Binoy Kumar Karmakar, Gopinath Karmakar. A Current Supported PV Array Reconfiguration Technique to Mitigate Partial Shading. IEEE Transactions on Sustainable Energy. 12 (2), 1449-1460, 2021.
[24] A. Srinivasan; S. Devakirubakaran; B. Meenakshi Sundaram; Praveen Kumar Balachandran et al. L-Shape Propagated Array Configuration With Dynamic Reconfiguration Algorithm for Enhancing Energy Conversion Rate of Partial Shaded Photovoltaic Systems. IEEE Access. 9, 97661-97674, 2021.
[25] Rupendra Kumar Pachauri; Isha Kansal; Thanikanti Sudhakar Babu; Hassan Haes Alhelou. Power losses reduction of solar PV systems under partial shading conditions using re-allocation of PV module-fixed electrical connections. IEEE Access. 9, 94789-94812, 2021.
[26] Abdelrahman M. Mohamed, Abou-Hashima M. El-Sayed, Yehia S. Mohamed, Husam A. Ramadan. Enhancement of Photovoltaic System under Partial Shading Conditions. EULC, ID: 9098346, Thesis. 2020.
[27] J. Prasanth Ram, Dhanup S. Pillai, Ye-Eun Jang, Young-Jin Kim. Reconfigured Photovoltaic Model to Facilitate Maximum Power Point Tracking for Micro and Nano-Grid Systems. Energies. 15 (23), 8860, 2022
[28] Aidha Muhammad Ajmal, Thanikanti Sudhakar Babu, Vigna K. Ramachandaramurthy, Dalia. Yousri, Janaka B. Ekanayake. Static and dynamic reconfiguration approaches for mitigation of partial shading influence in photovoltaic arrays. Sustainable Energy Technologies and Assessments, 40, 100738, 2020.
[29] Bo Yang, Haoyin Ye, Jingbo Wang, Jiale Li et al. PV arrays reconfiguration for partial shading mitigation: Recent advances, challenges and perspectives. Energy Conversion and Management, 247, 114738, 2021.
[30] Mariana Durango-Flórez, Daniel González-Montoya, Luz Adriana Trejos-Grisales, Carlos Andres Ramos-Paja. PV Array Reconfiguration Based on Genetic Algorithm for Maximum Power Extraction and Energy Impact Analysis. Sustainability. 14 (7), 3764, 2022.
[31] Vinaya Chandrakant Chavan, Suresh Mikkili, Tomonobu Senjyu. Hardware Implementation of Novel Shade Dispersion PV Reconfiguration Technique to Enhance Maximum Power under Partial Shading Conditions. Energies. 15 (10), 3515, 2022.

الملخص

تقل قيمة الطاقة الإجمالية الناتجة عن منظومة الطاقة الشمسية بشكل كبير عندما لا تتعرض الألواح لكميات متساوية من الإشعاع الشمسي. في هذه الدراسة تمت مقارنة ثلاث طرق مختلفة لزيادة انتاج الطاقة تحت تأثير هذه الظروف. استندت الأساليب الثلاثة إلى منهجيات مختلفة ؛ الساكنة وإعادة تشكيل العمود وإعادة تشكيل المصفوفة. تم تمثيل المنهجيات الثلاثة من خلال طرق TCT و CWR وRTCT على الترتيب. أثبت كل منها تفوقه على نظرائه باستخدام نفس المنهجية. تم اختبار الطرق الثلاث في جزأين. تضمن الجزء الأول خمسة أنماط تظليل ثابتة مختلفة وتم اختبارها على نظام 5 × 5. أظهرت RTCT نتائج متفوقة مقارنة بالطريقتين الأخريين. لقد حسّنت إنتاج الطاقة في جميع الأنماط الخمسة بمعدلات تتراوح بين 1.45٪ و 32.49٪. بينما حققت طريقة CWR تحسنًا في أربعة أنماط بنسب أقل (بين 1.68٪ و 27.81٪) ، وكان نمط واحد أقل من طريقة TCT. في الجزء الثاني ، تم اختبار الطرق الثلاث على نظام من مائة وحدة ، مرتبة في مصفوفة 10x10 ، وتحت نمط إشعاع شمسي ديناميكي يتغير بمرور الوقت في عشرة أنماط. قدمت RTCT أعلى معدل تحسن لجميع الحالات بنسبة 9.5 ٪ لمتوسط الفترة الإجمالية بينما حققت CWR 6.9٪. وبالتالي يوصى بالتطوير المباشر للأنظمة الساكنة الى نظام إعادة تشكيل المصفوفة باستخدام RTCT إذا كان الهدف هو الحصول على أقصى طاقة ممكنة. تم إجراء عمليات المحاكاة باستخدام برنامج MATLAB/Simulink ، حيث تم الحصول على المنحنيات المميزة وقيم الفولتية والتيارات والطاقة لكل حالة.